

Supplementary Information for

TRPA1 Ankyrin Repeat Six Interacts with a New Class of Inhibitor
Chemotype

Wei Chou Tseng¹, David C. Pryde², Katrina E. Yoger³, Karen M. Padilla³, Brett M.
Antonio³, Seungil Han⁴, Veerabahu Shanmugasundaram⁴, Aaron C. Gerlach³

Aaron Gerlach
Email: agerlach@icagen.com

This PDF file includes:

Supplementary text
Figs. S1 to S8
Tables S1

Supplementary Information Text

Materials and Methods

DNA Plasmids and cell lines

DNA representing full-length TRPA1 sequences from human (CAA71610), rat (NP_997491.1) and opossum (XP_001378427) were cloned into inducible vector pcDNA5/TO (Invitrogen). Gene synthesis and chimera production were performed by GenScript USA, site-directed mutagenesis was performed using QuickChange II (Agilent Technologies). Stable clonal cell lines were generated in 293-T-REx cell line (Invitrogen), selected with 150 µg/ml hygromycin and 5 µg/ml blasticidin and induced with tetracycline (1 µg/ml).

FLIPR assay

Stable cell lines were grown in 384 well poly-D-lysine coated tissue culture plates and loaded with 4 µM Fluo-4 AM (Invitrogen # F14217) for 45-60 minutes in Earls Balanced Salt Solution (EBSS, 132 mM NaCl, 5.4 mM KCl, 1.8 mM CaCl₂, 0.8 mM MgCl₂, 10 mM HEPES and 5 mM glucose) at room temperature. At the end of the incubation period, the Fluo-4 solution was removed and replaced with low Ca²⁺ EBSS containing 0.5 mM CaCl₂. Cells were pre-incubated for 5 minutes with test compounds prior to activation with 3 µM AITC or 1 µM PF-4840154. All additions and fluorescence measurements were carried out on a FLIPR 2 instrument (Molecular Devices) with excitation/emission wavelength of 490/520 nm.

Whole-Cell Patch Clamp Electrophysiology

Wild type and mutant TRPA1 channels were recombinantly expressed in T-Rex-293 cells (Thermo Fisher) and recorded. Whole-cell patch clamp recordings were obtained using patch pipettes with resistances of 1.5 to 2.5 MΩ when filled with the internal solution, consisting of (in mM) 90 CsCl, 32 CsF, 10 HEPES, 10 EGTA, 10 Cs₄ BAPTA, 1 MgCl₂, 5 Mg ATP, and 0.1 Na GTP, pH adjusted to 7.3 with CsOH. The external solution consisted of (in mM) 132 NaCl, 5.4 KCl, 1.8 CaCl₂, 0.8 MgCl₂, 10 HEPES, and 5 Glucose, pH adjusted to 7.4 with NaOH. 300 µM cinnamaldehyde was perfused to activate channels and test compounds applied in the continued presence of agonist. TRPV1 and TRPM8 channels were recorded in the same solutions but activated with 0.03 µM capsaicin and 100 µM menthol, respectively. All currents were recorded at room temperature with an Axopatch 200B amplifier (Molecular Devices) and filtered at 1 kHz with a low-pass Bessel filter. Voltage protocols were evoked every 5 second using the voltage protocols described in Fig. 2 The mean steady-state current at the -40 mv step (-50 mV for TRPM8) for each test concentration was analyzed using Clampfit 10.2 software (Molecular Devices).

Data Analysis and Curve Fitting

For FLIPR individual concentration responses were fitted with the Hill equation to determine IC₅₀, averaged and are reported as mean ± SEM. Compounds that produced <50% inhibition at 10 µM were not fit and are reported as IC₅₀>10 µM. For manual patch-clamp electrophysiology data, concentration-responses were normalized to vehicle control current. The individual percent inhibitions were then averaged for each test concentration and plotted as mean ± SEM. These data were fitted with the Hill equation to determine IC₅₀ and 95% confidence intervals (CI). For statistical analysis, ANOVA with *post hoc* Dunnett's *t*-test was applied with P<0.05 considered as statistically significant. All curve fitting and statistical analysis was performed using Prism 7.0 software (GraphPad).

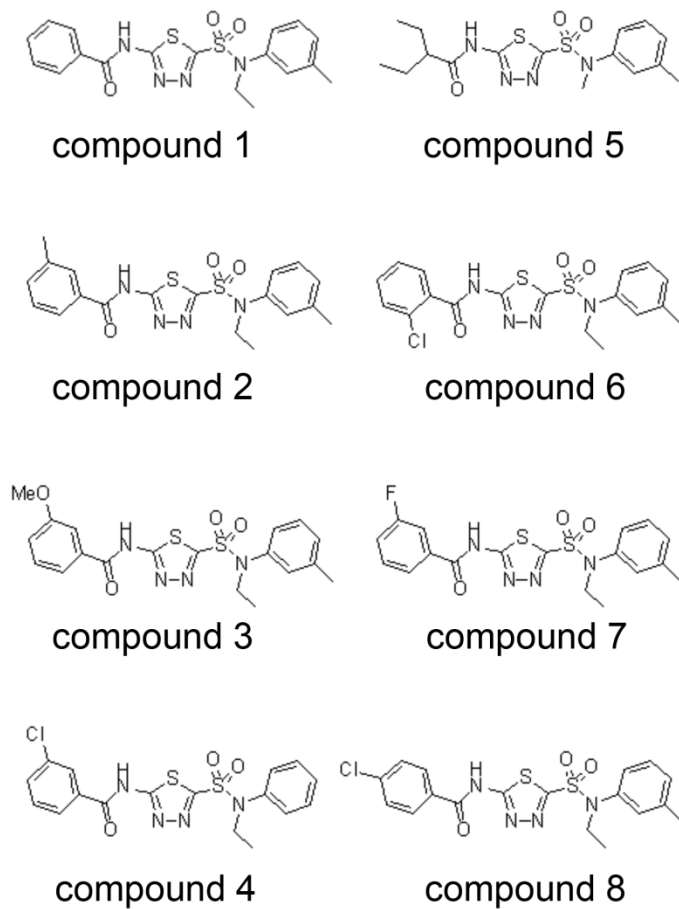


Fig. S1. Chemical structures of all reported thiadiazole series compounds

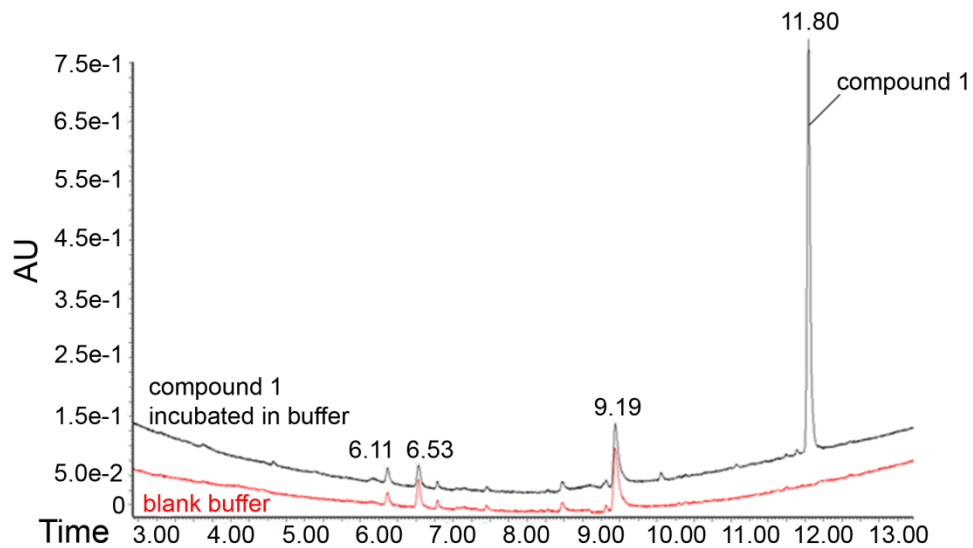


Fig. S2. Chemical stability of Compound **1**. Compound **1** (m/z 403) was incubated for 1hr (37°C, 25 μ M) in potassium phosphate buffer (100mM, pH 7.4) with additional glutathione (5mM) and the resulting samples analyzed by LC-UV/MS. Unchanged compound was identified following incubation in buffer, with no major breakdown products identified, indicating that Compound **1** was not subject to covalent capture and degradation by glutathione. The study was carried out by UniLabs – York Bioanalytical Solutions, Discovery Park, Ramsgate Road, Sandwich, CT13 9ND, UK.

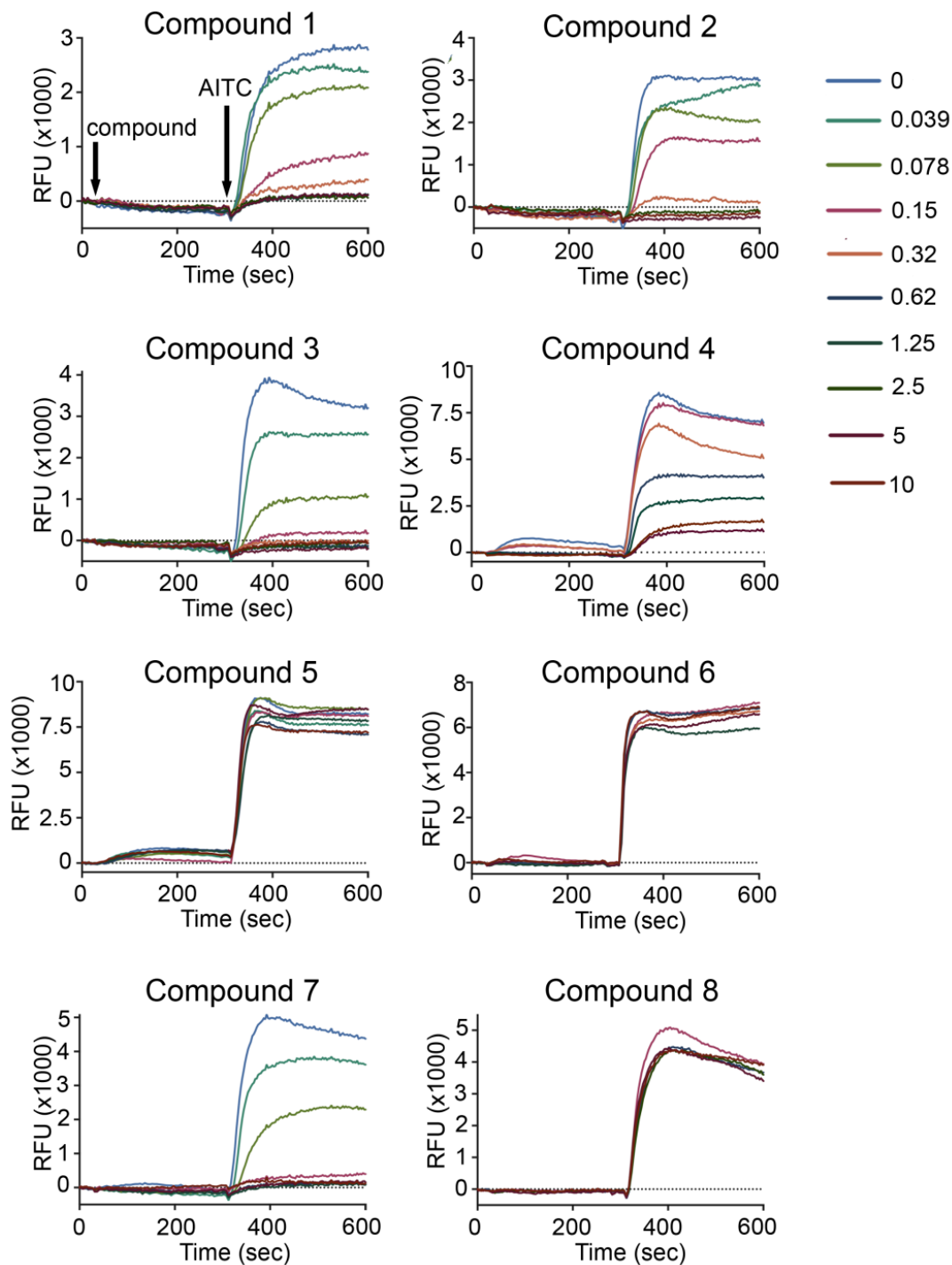


Fig. S3. Representative FLIPR traces showing thiadiazole effects on AITC activated human TRPA1. Shown are representative TRPA1 FLIPR traces supporting the SAR table shown in Figure 1C. Compounds were incubated for 5 minutes at increasing concentrations in 2-fold increments up to 10 μM. AITC (3 μM) was then added where indicated in the continued presence of test compound for an additional 5 minutes. Compound concentrations are in micromolar units on the color key.

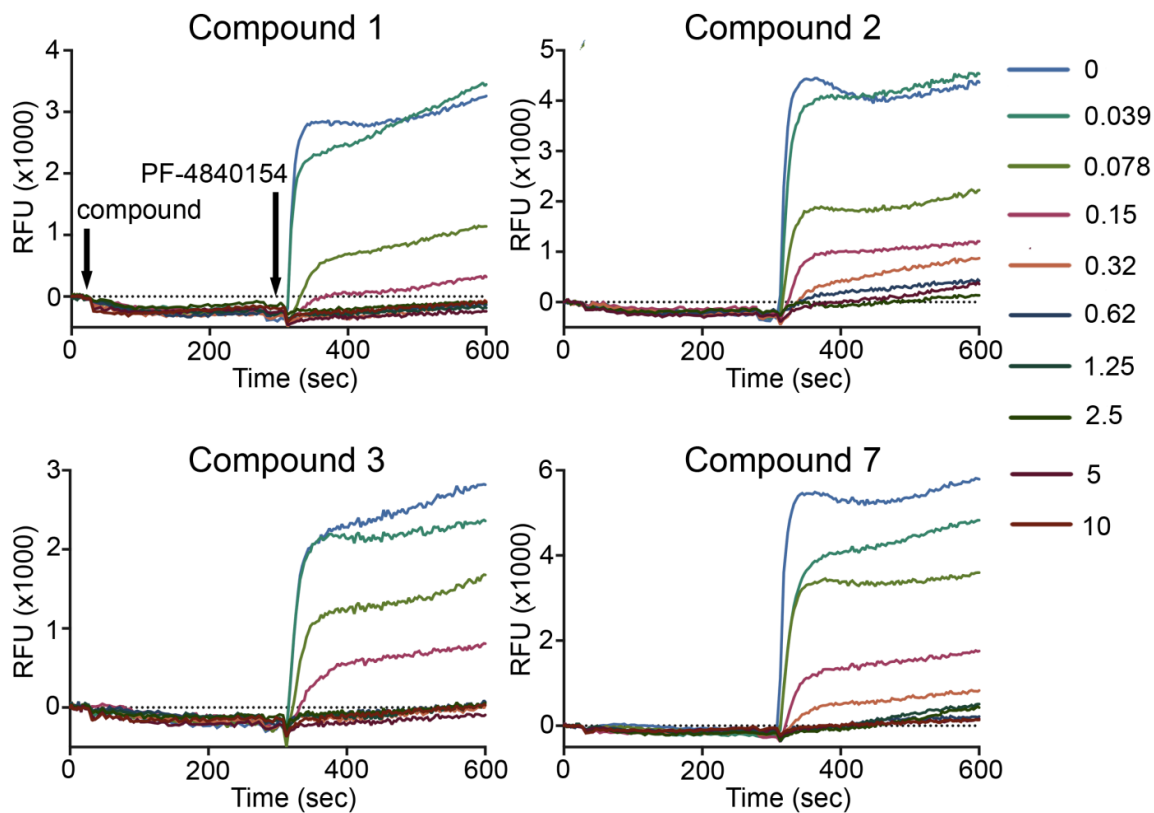


Fig. S4. Representative FLIPR traces showing thiadiazole effects on PF-04840154 activated human TRPA1. Shown are representative TRPA1 FLIPR traces of compound **1**, **2**, **3** and **7** effects on PF-4840154 activated channels. Unlike AITC, PF-4840154 is a non-electrophilic agonist. Compounds were incubated for 5 minutes at increasing concentrations in 2-fold increments up to 10 μM. PF-4840154 (1 μM) was then added where indicated in the continued presence of test compound for an additional 5 minutes. Compound concentrations are in micromolar units on the color key.

Table S1. TRP channel potency and selectivity in patch-clamp electrophysiology.

		Compound			
		1	2	3	7
hTRPA1	IC ₅₀ (μM)	0.13 ± 0.05	0.09 ± 0.02	0.11 ± 0.03	0.17 ± 0.03
	% Inhibition at 10 μM	98±2	100±3	99±2	99±4
rTRPA1	IC ₅₀ (μM)	>10	>10	>10	>10
	% Inhibition at 10 μM	12±2	3±7	8±3	0.2±6
hTRPV1	IC ₅₀ (μM)	>10	>10	>10	>10
	% Inhibition at 10 μM	-2±1	11±2	4±2	-3±2
hTRPM8	IC ₅₀ (μM)	>10	>10	>10	>10
	% Inhibition at 10 μM	4±4	14±5	8±3	17±3

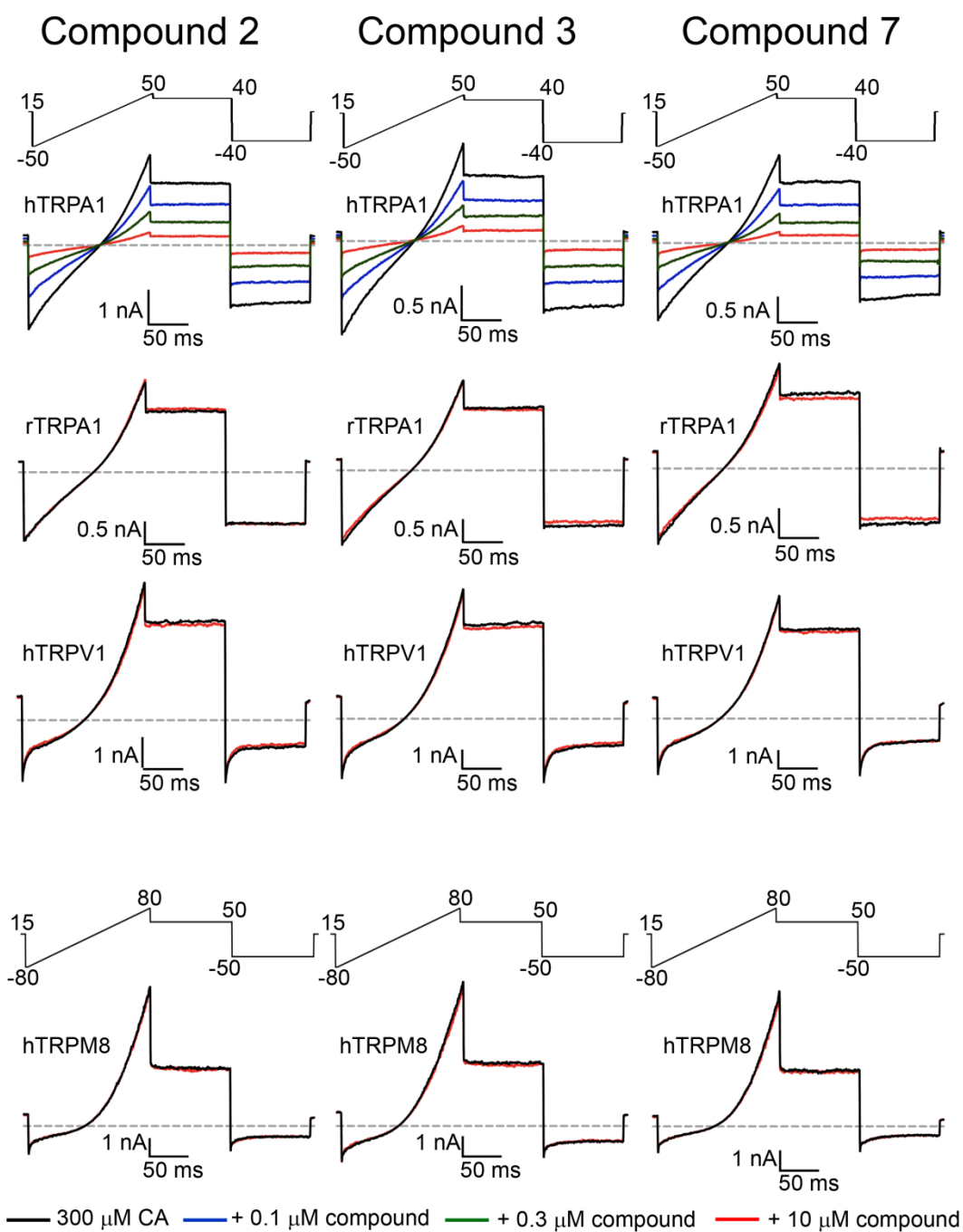


Fig. S5. Selectivity of compounds 2, 3 and 7. Shown are representative manual patch electrophysiology traces supporting the summarized results in Table S1. TRPA1 was activated by 300 μ M cinnamaldehyde (CA), TRPV1 by 0.03 μ M capsaicin and TRPM8 by 100 μ M menthol. After reaching steady-state, test compounds were co-applied. Protocols are the same as for compound 1 which is shown in figure 2A-B.

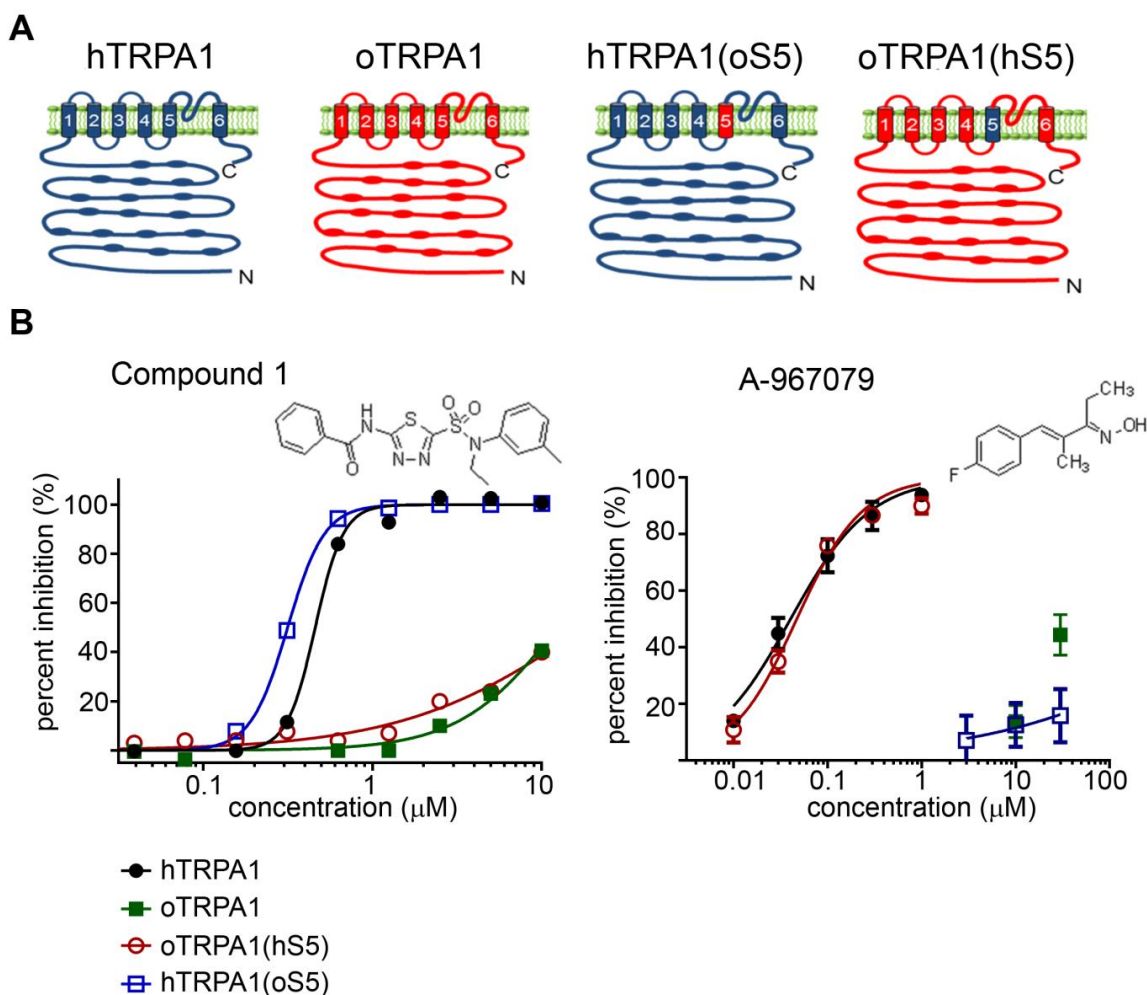


Figure S6. Compound **1** interaction is not dependent upon S5 pore helix (A) Schematics of chimeras in which the 21 amino acid S5 helix of human TRPA1 (hTRPA1) and opossum TRPA1 (oTRPA1) were interchanged. (B) Compound **1** potency was compared to A-967079 on chimeric hTRPA1 channels containing the opossum S5 helix, (hTRPA1(oS5)) and opossum TRPA1 chimeras containing the hTRPA1 S5 helix (oTRPA1(hS5)). Compound **1** (left) was selective for hTRPA1 over oTRPA1 channels and potency was not dependent on the hTRPA1 S5 helix. In contrast, A-967079 (right) potency was fully dependent upon the hTRPA1 S5 helix.

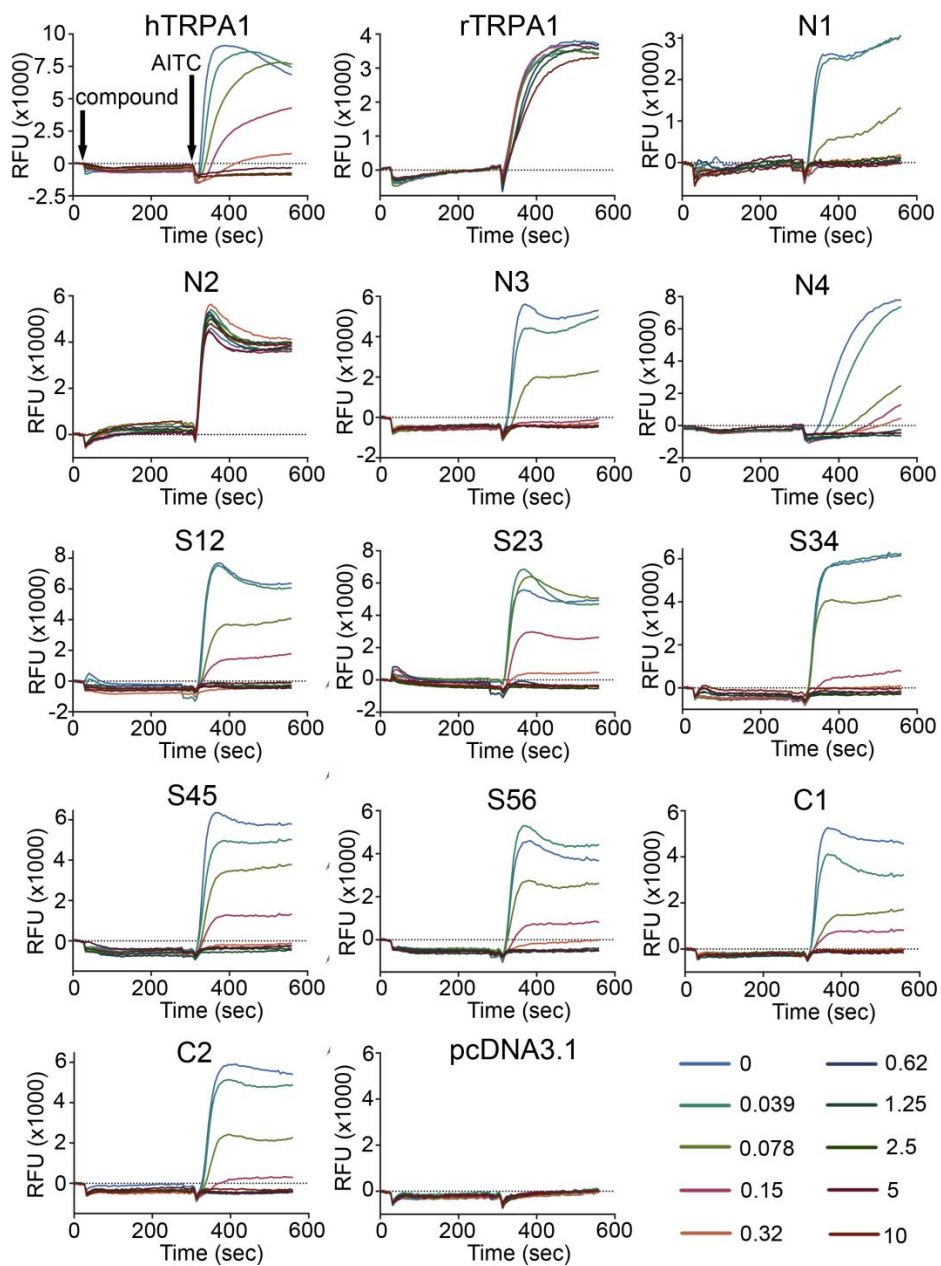


Figure S7. Representative FLIPR traces showing Compound **1** effects on human-rat TRPA1 chimeras. Representative FLIPR traces supporting Figure 2C-D summary data are shown. Compound **1** was incubated for 5 minutes at increasing concentrations in 2-fold increments up to 10 μM . AITC (3 μM) was then added where indicated in the continued presence of test compound for an additional 5 minutes. Compound concentrations are in micromolar units on the color key.

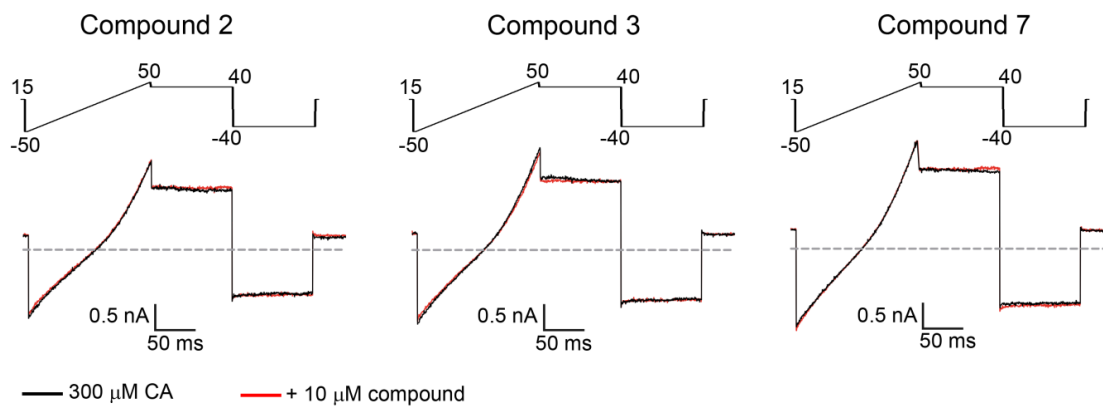


Figure S8. Effects of compounds **2**, **3** and **7** on hTriple mutant. Shown are representative hTriple mutant manual patch electrophysiology traces in response to 10 μM of compounds **2**, **3** and **7**. Channels were activated by 300 μM cinnamaldehyde (CA) and compounds did not show appreciable inhibition.